Toxicology Reports 9 (2022) 191–203

Contents lists available at ScienceDirect

Toxicology Reports

journal homepage: www.elsevier.com/locate/toxrep

Characteristics of a novel photoinitiator aceanthrenequinone-initiated polymerization and cytocompatibility of its triggered polymer

Yongjia Xiong [a,1], Hailing Zou [a,1], Shuhui Wang [a,1], Jiawen Guo [b], Boning Zeng [a], Pu Xiao [a,c,*], Jing Liu [d,**], Feiyue Xing [a,*]

[a] Institute of Tissue Transplantation and Immunology, Department of Immunobiology, MOE Key Laboratory of Tumor Molecular Biology, Jinan University, Guangzhou, 510632, China
[b] Guanghua School of Stomatology, Hospital of Stomatology, Sun Yat-sen University, Guangzhou, 510055, China
[c] Research School of Chemistry, Australian National University, Canberra, ACT, 2601, Australia
[d] School of Stomatology, Jinan University, Guangzhou, 510632, China

ARTICLE INFO

Handling Editor: Dr. Aristidis Tsatsakis

Keywords:
Aceanthrenequinone
9,10-phenanthrenequinone
Photopolymerization
Biocompatibility
Cytotoxicity

ABSTRACT

A number of photoinitiators are available in chemical industry, but less of them in biomedicine or clinical therapy due to the limitation of their cytotoxicity and biocompatibility. Thus, it is urgently necessary to find non-toxic or low-toxic photoinitiators to meet clinical demands. Aceanthrenequinone (AATQ) is a novel photosensitizer with high-photoinitiating ability, but no reports contribute, to date, to its cytotoxicity and biocompatibility. Here, primary cells and various cell lines were exposed to different concentrations of AATQ with or without irradiation. AATQ had the similar photoinitiating conversion efficiency to the extensively used bis(2,4,6-trimethylbenzoyl)-phenylphosphine oxide (BAPO) and higher one than 9,10-phenanthrenequinone (PANQ) with the similar extent of polymerization in depth within a certain range, but displayed much lower cytotoxicity than BAPO under non-irradiation or irradiation. The biocompatibility of BisGMA/TEGDMA polymer prepared by AATQ was superior to that of PANQ, but inferior to that of camphorquinone (CQ) although the far lower dose of AATQ is enough to initiate polymerization of monomer than that of CQ. Hence, AATQ offers a valuable alternative in applications of industrial or biomedical areas.

1. Introduction

Photopolymerization is widely used in industrial fields, particularly coating, printing and optical materials [1] and now increasingly applied to preparation of biomedical materials, such as adhesives, sealants, controlled release and tissue engineering scaffolds, and in clinical therapy, such as dental and articular cartilage restoration. Photoinitiator is a key component in a photopolymerization system. It generates ions or free radicals under the irradiation of visible light or ultraviolet light to initiate polymerization, crosslinking and curing of monomers. According to the mechanism of photoinitiation, photoinitiators are divided into two types: free radical photoinitiators and cationic photoinitiators. Besides photoinitiators, monomers or oligomers also play important roles in the photopolymerization system. For example, poly(methyl methacrylate) (PMMA)-based appliances can be used to withstand the mechanical and microbial harm in the oral cavity. The resistance of photoinitiated-repair resin to dental friction and wear may be enhanced by the incorporation of nanodiamond into PMMA [2]. Photo-crosslinkable methacrylated gelatin is copolymerized with acrylamide to form a polymer biohybrid hydrogel in the presence of a photoinitiator with ultraviolet radiation, improving the articular cartilage repair *in vivo* [3]. Alginate hydrogels are also employed in cell encapsulation, cell transplantation and tissue engineering [4], and can form a double cross-linked network under photo-cross-linking activated by visible light and ultraviolet light [5]. A three-component system based on an interpenetrating polymer network of gelatin, alginate and polyacrylamide induces the transformation of human adipose-derived stem cells into functional chondrocytes [6]. The findings and practices hint that these materials might have great potential in tissue and soft tissue engineering applications.

* Corresponding authors at: Institute of Tissue Transplantation and Immunology, Department of Immunobiology, Jinan University, Guangzhou, 510632, China.
** Corresponding author.
E-mail addresses: twxiao@jnu.edu.cn, pu.xiao@anu.edu.au (P. Xiao), tjliu@jnu.edu.cn (J. Liu), tfyxing@jnu.edu.cn (F. Xing).
[1] These authors contributed equally to this work.

https://doi.org/10.1016/j.toxrep.2022.01.008
Received 22 August 2021; Received in revised form 13 December 2021; Accepted 25 January 2022
Available online 28 January 2022

Although a large number of photoinitiators are available, most of them have insufficient photoreactivity with poor water solubility and biocompatibility not to meet environmental and clinical demands. In clinical, the most significant polymer can be obtained under dental resin polymerization initiated by camphorquinone (CQ), which is type II radical photoinitiator. The photopolymerization reactant diffuses gradually into human body through direct contact or residual, hereby causing undesirable systemic reactions. Therefore, it is necessary to find and develop some photoinitiators having good photochemical properties and high polymerization efficiency with low toxicity, especially cytocompatibility and tissue compatibility. Aceanthrenequinone (AATQ) is early used in a variety of organic synthesis or as a chemical material intermediate [7–9], but no reports is, to date, involved in cytotoxicity and cytocompatibility of itself and its-initiated polymer on mammalian cells. Moreover, some studies have shown that AATQ is simultaneously a component of vehicle exhaust emissions and PM2.5 [10,11], suggesting that it could have potentially adverse effects on human body, but no toxicology parameters have been reported. Therefore, it is of great significance to explore its cytotoxicity and compatibility for its potential application in biomedicine.

2. Materials and methods

2.1. Chemicals

Bisphenol A glycerolate dimethacrylate (Bis-GMA), aceanthrenequinone (AATQ), triethanolamine (TEAOH), phenacyl bromide (R-Br) and 9,10-phenanthrenequinone (PANQ) were obtained from Sigma-Aldrich. Investigated bis(2,4,6-trimethylbenzoyl)-phenylphosphine oxide (BAPO), camphorquinone (CQ), diphenyliodonium hexafluorophosphate (Iod), ethyl 4-(dimethylamino) benzoate (EDB) and triethylene glycol dimethacrylate (TEGDMA) were ordered from Aladdin (Fig. 1).

2.2. Cell isolation and culture

Human embryonic kidney 293T cell line HEK293T, human umbilical vein endothelial cell line HUVEC-12, human normal hepatocyte line LO-2 were preserved in our laboratory. All cells were cultured with Dulbecco's Modified Eagle's Medium (DMEM, Gibco, USA) containing 10 % (v/v) fetal bovine serum (FBS, Gibco, USA) at 37 °C in a 5 % CO2 incubator. 8- to 10-week-old male C57BL/6 mice were provided by the Guangdong Medical Animal Center (Guangzhou, China). The protocol was approved by Jinan University Experimental Animal Ethics Committee. Bone marrow stromal cells (BMSCs) were separated from the mice according to the reported method [12,13]. The isolated cells were

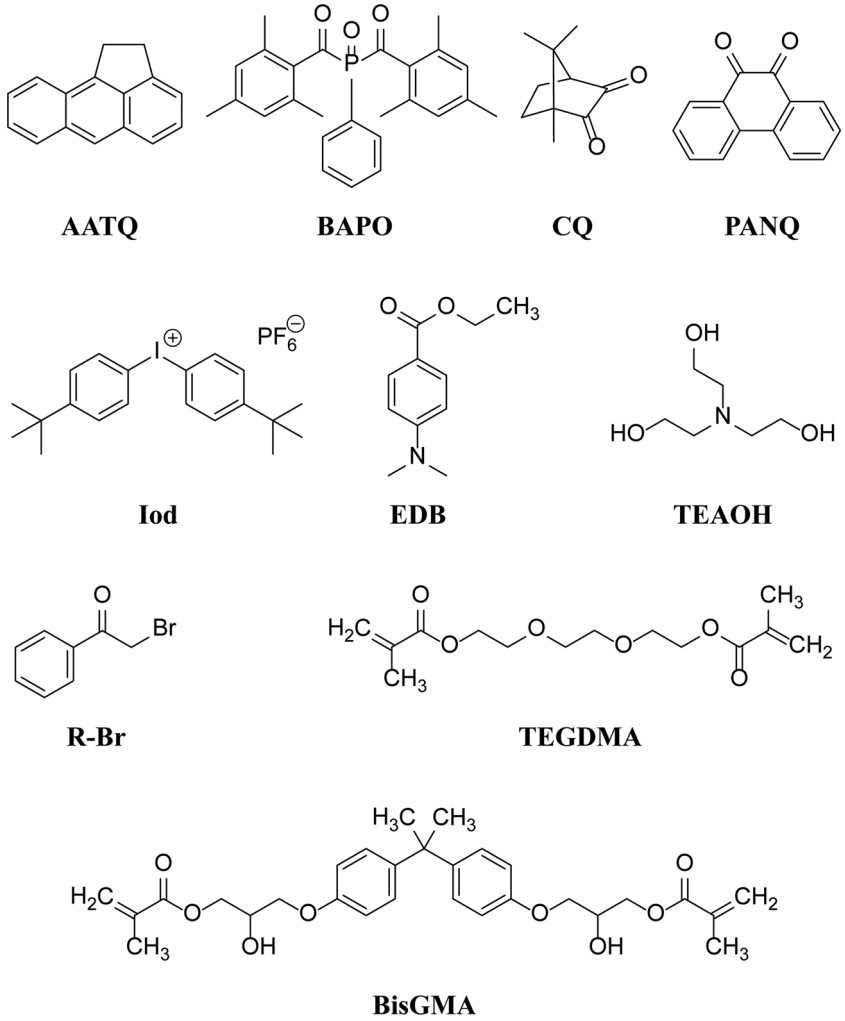

Fig. 1. Chemical structures of the photoinitiators (AATQ, BAPO, CQ, PANQ), additives (EDB, Iod, TEAOH, R-Br) and monomers (BisGMA, TEGDMA) used in this study. AATQ, aceanthrenequinone; BAPO, bis(2,4,6-trimethylbenzoyl)-phenylphosphine oxide; CQ, camphorquinone; PANQ, 9,10-phenanthrenequinone; EDB, ethyl 4-(dimethylamino) benzoate; Iod, diphenyliodonium hexafluorophosphate; TEAOH, triethanolamine; R-Br, phenacyl bromide.

resuspended in DMEM supplemented with 10 % fetal bovine serum at 37 °C in a 5% CO2 incubator for culture.

2.3. MTT assay

Cytotoxicity of AATQ was tested by 3-(4,5-dimethylthiazol-2-yl)-2,5-diphenyltetrazolium bromide dye (MTT) under irradiation and non-irradiation conditions. 1×10^4 cells/well was seeded onto 96-well plates with 100 μL of medium per well and incubated for 24 h, respectively. Photoinitiator AATQ and positive control BAPO were dissolved with dimethyl sulfoxide (DMSO) to prepare high-concentration storage solutions, which were kept away from light, and diluted with DMEM to 5, 10, 25, 50, and 100 μM. The cells were then exposed to different concentrations of the photoinitiators, respectively. The plates were exposed to 455 nm blue light for 5 min before further 24 -h incubation. Then, they were photographed under an inverted microscope. 10 μL MTT at the final concentration of 0.5 mg/mL was added to each well and the cells were incubated for additional 4 h. The formed formazan crystals were dissolved in DMSO. Finally, optical density (OD) was measured at 570 nm by a microplate reader (Multiskan FC, Thermo, China).

2.4. Flow cytometry analyses

PI/Annexin V-FITC Apoptosis Detection Kit (KeyGEN, Nanjing, China) was harnessed for determining apoptotic and necrotic cells under irradiation and non-irradiation conditions in accordance with the manufacturer's instructions. In brief, 2×10^5 HEK293T cells/well was seeded onto 6-well microplates. After incubated with photoinitiators at 5, 10, 25, 50, and 100 μM for 24 h, the cells were blown down gently with a pipette, harvested into a centrifuge tube, and washed with cold PBS. Afterwards, 500 μl binding buffer, 5 μl annexin V and 5 μl PI were added to the cells. They were kept at room temperature in the dark for 10 min and finally tested as soon as possible on a flow cytometer (Attune NxT, Life Technologies, USA). 10, 000 events were tested for each sample. The data were analyzed by FlowJo V10 software, and the apoptosis rate of cells was analyzed by GraphPad software.

2.5. Photoinitiating conversion efficiency of AATQ

Measurement of conversion efficiency of the used photoinitiators AATQ, PANQ, BAPO and CQ was conducted in laminated conditions. The photosensitive formulations were deposited on 25 μm thick of a BaF2 pellet exposed to 455 nm LED light. Evolution of the double bond content of BisGMA/TEGDMA (70 %/30 %, wt %) blend was followed by Fourier Infrared Spectroscopy (Invernio R, Bruker, USA) at about 1635 cm^{-1}.

2.6. Preparation of AATQ-initiated polymer

AATQ/EDB (0. 5 %/1 %, wt %), AATQ/EDB (0.05 %/1 %, wt%), PANQ/TEAOH/R-Br (0.5 %/2 %/3 %, wt%) or CQ/EDB(0.5 %/1 %, wt %) were dissolved in BisGMA:TEGDMA (70:30 wt ratio) to prepare the prepolymer solutions. The precursor solution was pipetted into a mold defined with both photo-permeable glass slides separated by a silicone rubber spacer. The mixture was then irradiated under blue LED (455 nm) for 5 min.

2.7. Extent of polymerization in depth of AATQ

The extent of polymerization in depth was mapped by hardness testing. 4 × 4 mm bar-shaped specimens of 25 mm in length were prepared by inserting distinct resins into custom-made Teflon molds. The 4 × 25 mm exterior surface facing upward was convenient for packing the resin into the cavity. A piece of glass slide was attached to the 4 × 4 mm face firmly. Irradiation was delivered only on the 4 × 4 mm surface of the sample facing the curing-light. Irradiance of 1200 mW/cm2 reached the surface of the tested specimen. After 10-minute curing, the bar-shape specimen was taken out to form the mold by removing the uncured part. Polished with 2000 grit sandpaper under copious water cooling, the hardness testing was carried out on the 4 × 25 mm surface (Struers Durascan-20, Struers, Denmark). Vickers hardness (HV) was measured from the end closest to the curing light source to the far end. Nine depths were selected with the incremental of 1 mm for each specimen. And two measurements were made per depth. Subsequently, HV values, % of maximal hardness, were calculated by the below equation, indicating the extent of polymerization.

$$\text{Extent of polymerization (\%)} = \text{Measured hardness/Maximum hardness}$$

2.8. Cytotoxicity of AATQ-initiated polymer extract

Each polymer was incubated at 37 ° C in 650 μl DMEM according to the international standard ISO 10993-12 to obtain extracts of 1 day and 7 days. Extracts were evaluated at five concentrations of 100, 50, 25, 10, and 1%. After attached in 96-well plates, 2.5×10^4 HEK293T cells/well was treated with various concentrations of extracts 100 μL per well and incubated for 24 h. Subsequently, MTT assay was done as described above and live/dead staining were performed, respectively. Cell viability was tested by using a Live & Dead Viability/Cytotoxicity Assay Kit for Animal Cells (KeyGen Biotech, Nanjing, China) in term of the manufacturer's instructions. The cells were stained with 2 μM calcein AM and 8 μM PI in PBS at 37 °C for 30 min before imaged under an inverted fluorescence microscope (Zeiss Axio Observer D1, Germany).

2.9. Cytocompatibility of AATQ-triggered polymer

5×10^4 HUVEC-12 cells/well was seeded into a 48-well plate containing AATQ- or CQ-triggered polymer before cultured in an incubator for 24 h. Cell growth on the surface of the polymer was determined by MTT assay at 570 nm under a microplate reader (Thermo scientific, Multiskan FC, Shanghai, China). Then, live/dead staining was performed for further testing cell viability as described above.

2.10. Statistical analysis

Statistical analysis was conducted by one-way ANOVA with Tukey's post-hoc test. Presented data come out from 3 independent experiments, appearing as mean ± standard deviation (SD). A p-value of < 0.05 was considered statistically significant.

3. Results

3.1. Comparison of photoinitiating conversion efficiency and polymerization extent by AATQ

Thin films of a Bis-GMA/TEGDMA blend (70 %/30 % w/w) were exposed to LED light at 455 nm through distinct photoinitiating systems. An excellent polymerization was obtained in CQ/EDB system (~60 % of conversion for 300 s of irradiation). On the contrary, 0.5 %PATQ/2 % TEAOH/3 %R-Br achieved a low conversion (33.11 ± 0.77 %) in the same conditions, whereas the final conversion of 0.1 %PATQ/2 % TEAOH/3%R-Br was 19.47 ± 0.15 %. BAPO and AATQ/EDB systems had the similar conversion rate with maximum average values of 52.11 ± 2.37 %, and 52.49 ± 0.61 %, respectively. In addition, AATQ/EDB system exhibited higher photoinitiation efficiency than PATQ/TEAOH/R-Br system under the 455 nm LED irradiation with the similar extent of polymerization in depth within a certain range (Fig. 2A).

As shown in Fig. 2B and C, the value represents the degree of curing. From 1–9 mm away from the light source, the deeper the color band is, the better the surface curing depth is. The results indicate that AATQ has

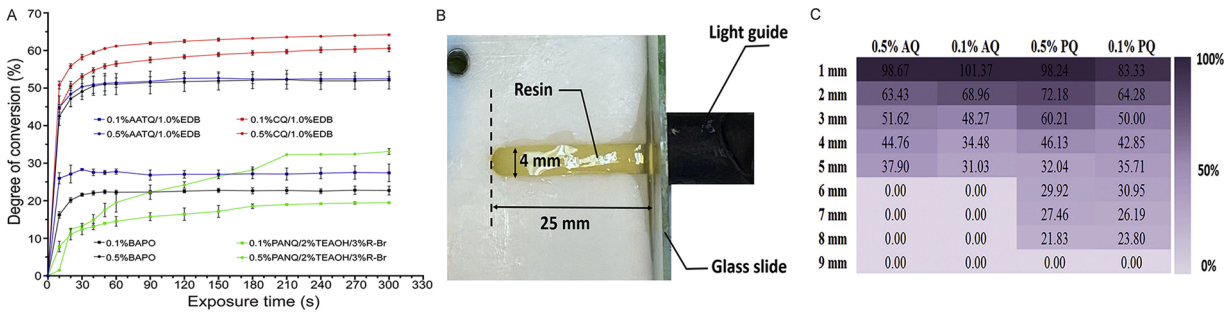

Fig. 2. Comparison of photoinitiating conversion efficiency and polymerization extent of AATQ with PANQ. A. Measurement of conversion efficiency of the used photoinitiators AATQ, PANQ, BAPO and CQ was carried out by Fourier Infrared Spectroscopy in laminated conditions at 455 nm blue LED. B. The extent of polymerization in depth was mapped by hardness testing. Bar-shaped specimens (4 mm × 4 mm) of 25 mm in length were produced by inserting the different resins in custom-made Teflon molds. C. Vickers hardness (HV) was measured from the end closest to the curing light source to the far end, and HV values % of maximal hardness were calculated, indicating the extent of polymerization. The mean values at each depth were used to build a 2D heat map as function of depth. (For interpretation of the references to colour in this figure legend, the reader is referred to the web version of this article).

the similar curing depth to PANQ within a certain range, compared to the corresponding concentration.

3.2. AATQ slightly represses some cell growth under non-irradiation

Figs. 3 and 4 show the results of MTT assay for four cell types of BMSCs, LO-2, HUVEC-12, HEK293T and exposed to AATQ or BAPO without irradiation, respectively. Compared with the control, BAPO could remarkably inhibit the proliferations of HEK293T, LO-2 and BMSCs in a concentration-dependent manner. The cell survival rate was just 19.0 ± 6.4 % at 100 μM, which shows its great cytotoxicity. However, the AATQ-treated survival cells remained 82.0 ± 9.7 % at 100 μM. AATQ also presented slight toxicity to HEK293T, LO-2 and BMSCs except HUVEC-12 cells, but it is much less than the commonly used BAPO because the overall survival rate was too higher than that of BAPO. In addition, HEK293T cells seemed to be more sensitive to AATQ or BAPO. Hence, the results indicate that AATQ has a certain inhibitory effect on cell growth at high concentrations.

3.3. Cytotoxicity of AATQ is much lower than BAPO under irradiation

Compared with non-irradiation, the cytotoxicities of BAPO to the four tested cells were largely increased under irradiation with the decreased relative survival rate of each type of cells. HEK293T cells seemed to be more sensitive to BAPO as well. The cytotoxicity of AATQ also became evident at the concentrations of 50, and 100 μM with irradiation and its survival rate was decreased to 76.6 ± 9.9, and 68.2 ± 7.6 %, but that of BAPO to 28.1 ± 9.0, and 16.2 ± 5.4 %, respectively. The sensitivity of the cells was the same as that of the non-irradiation group (Figs. 5 and 6). Thus, exposure of different types of the cells to activated AATQ promotes cell damage, but the cytotoxicity of AATQ is much lower than BAPO.

3.4. AATQ-induced cell apoptosis is far less than BAPO, but higher than CQ

At the lower concentrations of AATQ and BAPO, only a small percentage of cells were undergoing apoptosis and necrosis. AATQ and BAPO induced cytotoxicity in a dose-dependent manner after treated for 24 h, consistent with the results of the MTT assay. BAPO presented the similar effects on the cells when exposed to irradiation or not, inducing more pronounced cytotoxicity over the entire concentration range. Its treated cells appeared massively necrotic, suggesting a strong cytotoxic effect. AATQ slightly increased apoptotic cells at 5, and 10 μM. When cells were treated with 100 μM AATQ, the percentage of cells in Q2 and Q3 quadrants was slightly increased to 20.0 % and 19.1 %, respectively, indicating the increased apoptotic cell death (Fig. 7). Therefore, the proportion of AATQ-induced cell necrosis is far lower than BAPO under irradiation.

The activity of HEK293T cells treated by the composite extracts from AATQ- or CQ-initiated polymer is presented in Fig. 4. Compared with the control, the 1- or 7-day extract from CQ-triggered polymer scarcely influenced the cell growth by MTT and live/dead staining. The 1-day original extract from AATQ-triggered polymer slightly damaged the cells, causing 10 % of the cell death, but the 7-day original extract from AATQ-triggered polymer reduced the activity of the cells to 35.6 ± 9% (Fig. 8). The above results suggest that AATQ-initiated polymer may damage cell growth.

3.5. Cytocompatibility of AATQ-initiated polymer is superior to PANQ

HUVEC-12 cells grew on the surface of the polymer for 24 h. Similar to the control, the cell viability in the CQ group was near 100 % (Fig. 9). The cells appeared basically polygonal and spread well on the surface of the polymer. Moreover, the cell proliferation of CQ-triggered polymer was similar to that of the control. The polymer triggered by PANQ showed strong cytotoxicity, and thereon the cells all died without proliferation. The cells on the surface of the AATQ-triggered polymer appeared gradually rounded with some living cells and there was no statistical difference between its two doses. Therefore, the cytocompatible feature of the AATQ-triggered polymer is superior to PANQ, but inferior to CQ.

4. Discussion

Whether in food packaging materials, coatings or dentistry, use of toxic photoinitiators is a potential threat to human health. It has been reported that unreactive ingredients in dental resin can release into mouth during and after polymerization [14]. Among the photoinitiating systems, CQ is the most commonly used in dental resins, but it can damage aesthetic remediation because CQ is yellow-colored and amines turn yellow over time. Generally, 0.17–1.03 % w/w of CQ is usually used in polymerization of dental resin [15]. Studies have shown that CQ has obvious genotoxic potential in L5178Y/TK +/- mouse lymphoma cells probably due to intracellular reactive oxygen species (ROS)/reactive nitrogen species (RNS) production mediated by CQ [16]. Meereis et al. proposed that BAPO is a promising alternative for free radical polymerization of halogen-activated methacrylate monomers, which have properties similar to those conventionally used (CQ + EDAB), and the ternary system BAPO1 + EDAB + DPIHFP can produce the higher polymerization rate and the conversion degree [17]. Popal et al. subsequently studied the cytotoxicity/genotoxicity of 1–50 μM of BAPO or TPO to human oral keratinocytes (OKF6/Tert2) and Chinese hamster pulmonary fibroblasts (V79) [18,19]. The results showed that BAPO and

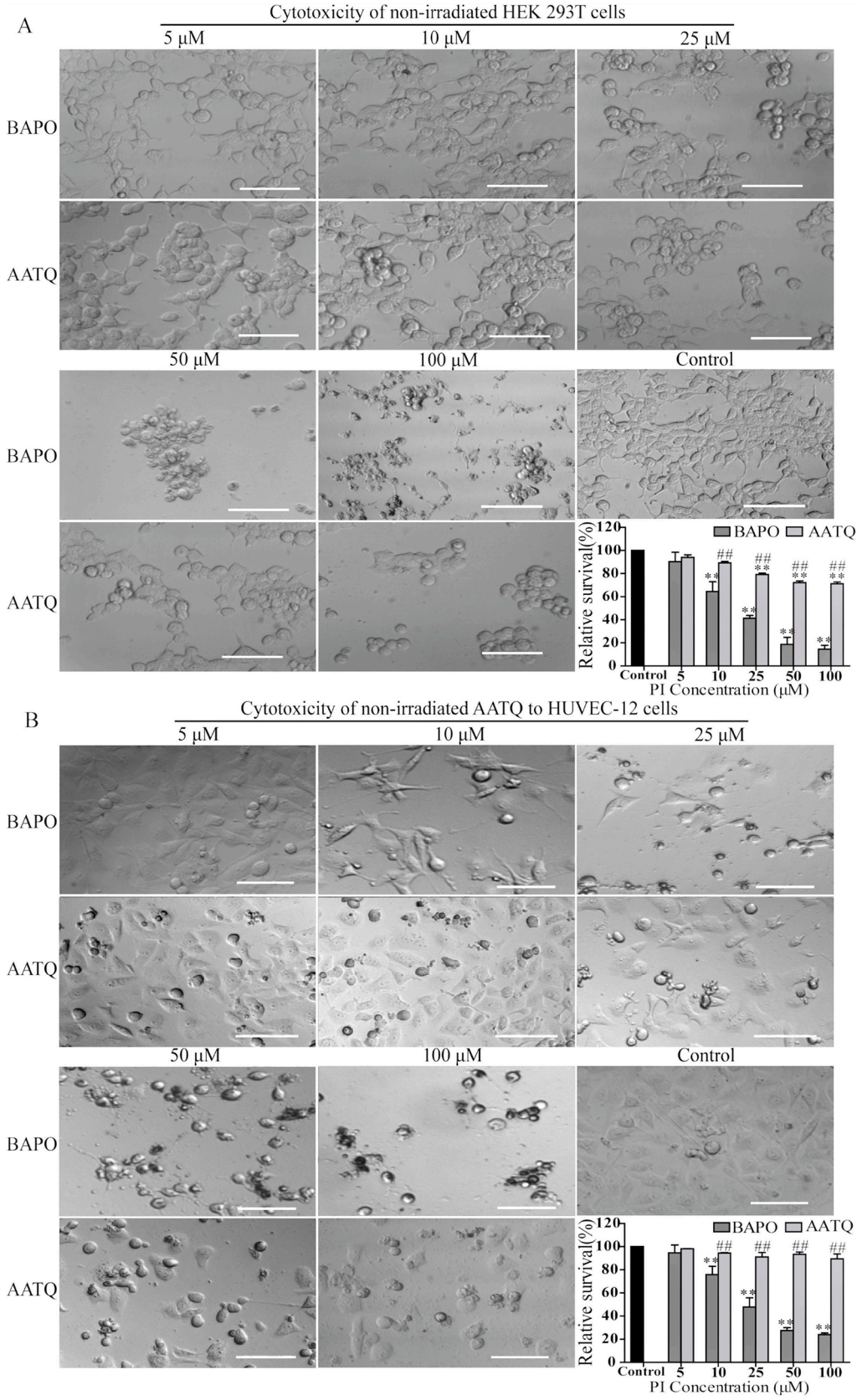

Fig. 3. Cytotoxicity of the non-activated AATQ to HEK293T and HUVEC-12 cells. HEK293T (A) or HUVEC-12 (B) cells were treated with 5-100 μM AATQ or BAPO for 24 h without irradiation, respectively. Cytotoxicity was assessed by the MTT assay. All values are presented as % of the solvent control. Statistical significance was analyzed using the Tukey test, $^{*}p < 0.05$, $^{**}p < 0.01$ *vs.* the control; $^{\#}p < 0.05$, $^{\#\#}p < 0.01$ *vs.* the BAPO group; Rulers in images: 100 μM.

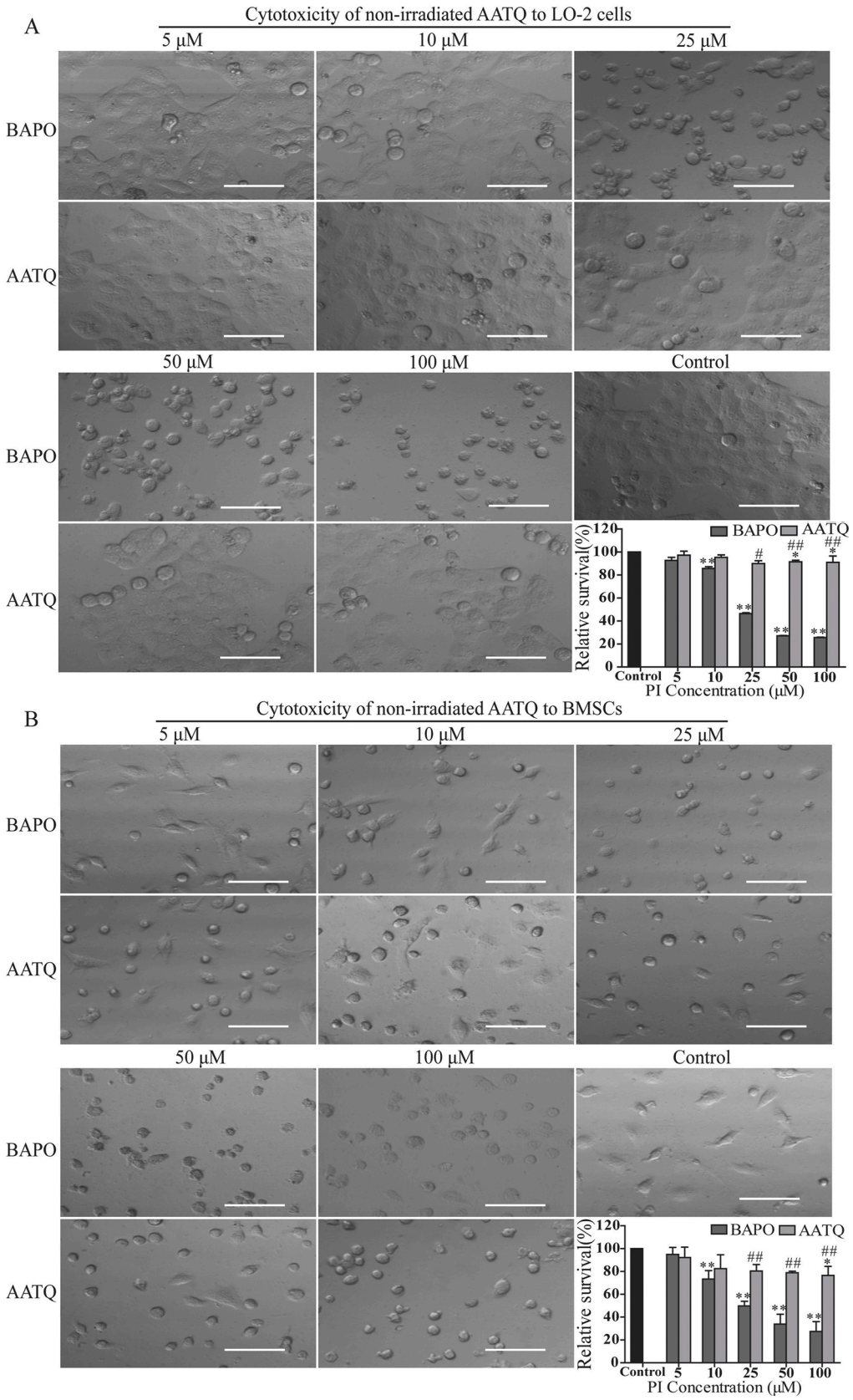

Fig. 4. Cytotoxicity of the non-activated AATQ to LO-2 cells and BMSCs. LO-2 cells (A) or BMSCs (B) were treated with 5-100 μM AATQ or BAPO for 24 h without irradiation, respectively. Cytotoxicity was assessed by the MTT assay. All values are presented as % of the solvent control. Statistical significance was analyzed using the Tukey test, $^{*}p < 0.05$, $^{**}p < 0.01$ *vs*. the control; $^{\#}p < 0.05$, $^{\#\#}p < 0.01$ *vs*. the BAPO group; Rulers in images: 100 μM.

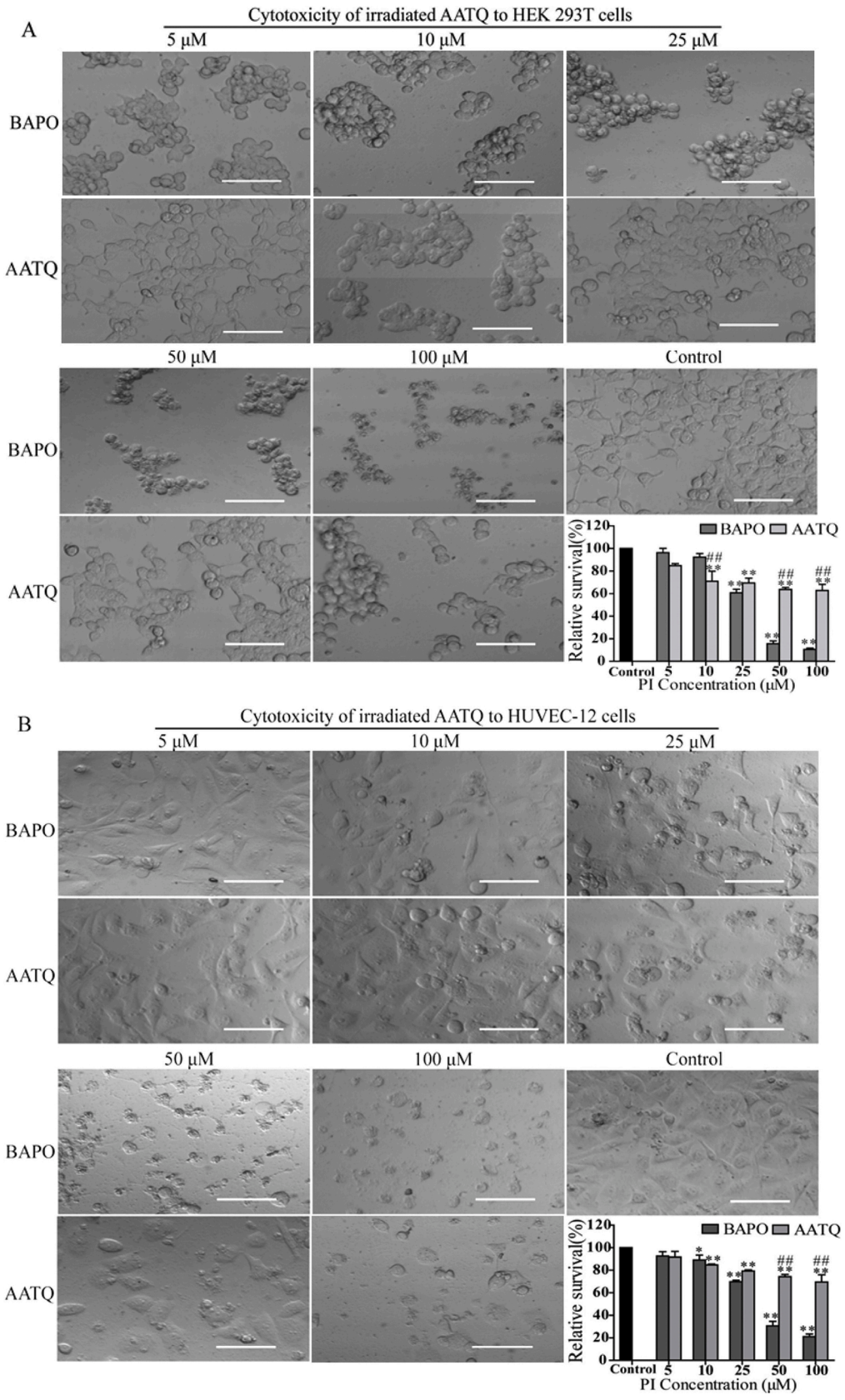

Fig. 5. Cytotoxicity of the activated AATQ to HEK293T and HUVEC-12 cells. A-B. After irradiated by blue LED (455 nm;100 mW cm-2) for 5 min, HEK293T (A) or HUVEC-12 (B) cells were treated with 5-100 μM AATQ or BAPO for 24 h. All values are presented as % of the solvent control. Statistical significance was analyzed using the Tukey test. $^{*}p < 0.05$, $^{**}p < 0.01$ *vs.* the control; $^{\#}p < 0.05$, $^{\#\#}p < 0.01$ *vs*. the BAPO group; Rulers in images: 100 μM. (For interpretation of the references to colour in this figure legend, the reader is referred to the web version of this article).

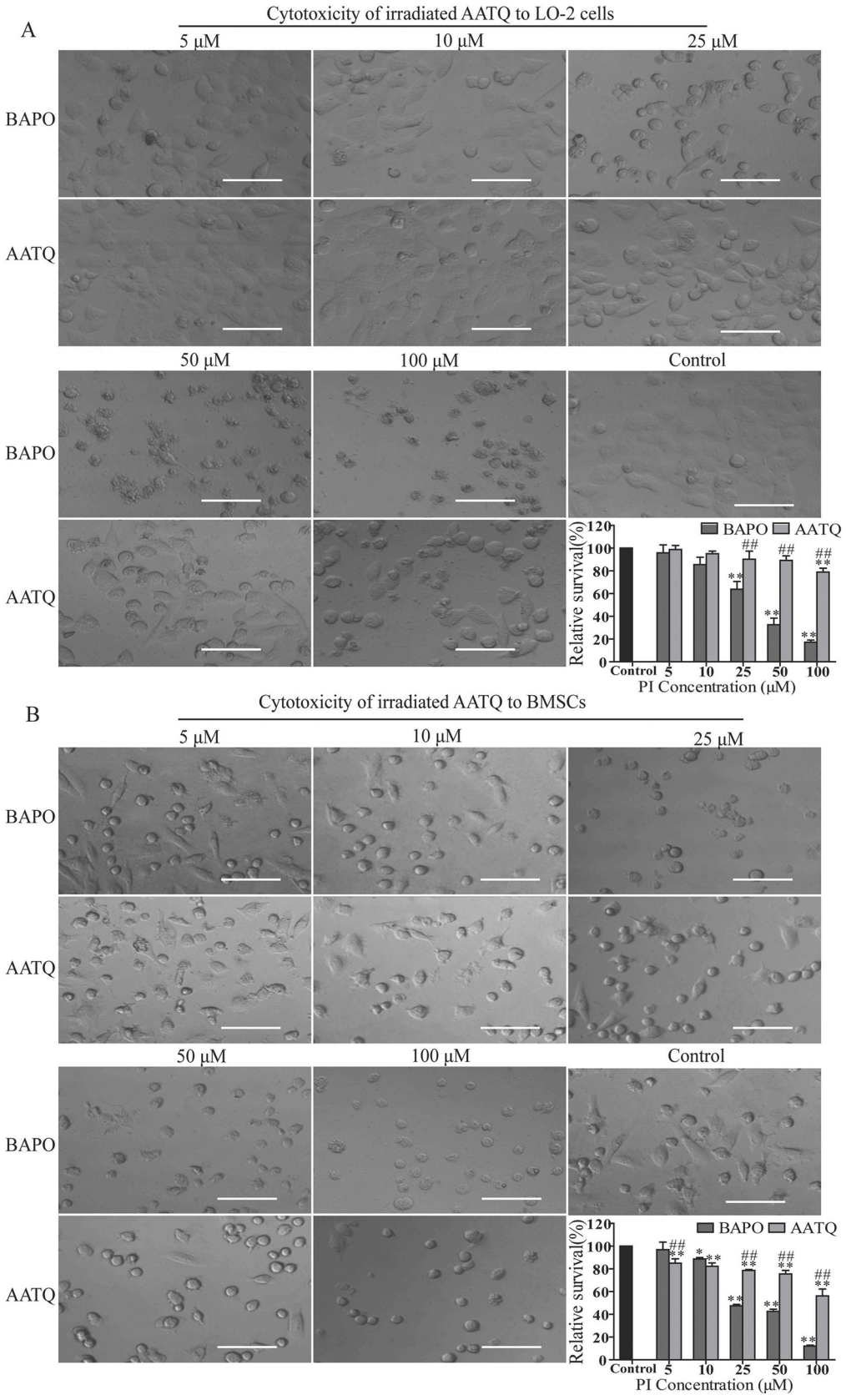

Fig. 6. Cytotoxicity of the activated AATQ to LO-2 cells and BMSCs. A-B. After irradiated by blue LED (455 nm;100 mW cm-2) for 5 min, LO-2 cells (A) or BMSCs (B) were treated with 5-100 μM AATQ and BAPO for 24 h. All values are presented as % of the solvent control. Statistical significance was analyzed using the Tukey test. $^{*}p < 0.05$, $^{**}p < 0.01$ *vs.* the control; $^{\#}p < 0.05$, $^{\#\#}p < 0.01$ *vs.* the BAPO group; Rulers in images: 100 μM. (For interpretation of the references to colour in this figure legend, the reader is referred to the web version of this article).

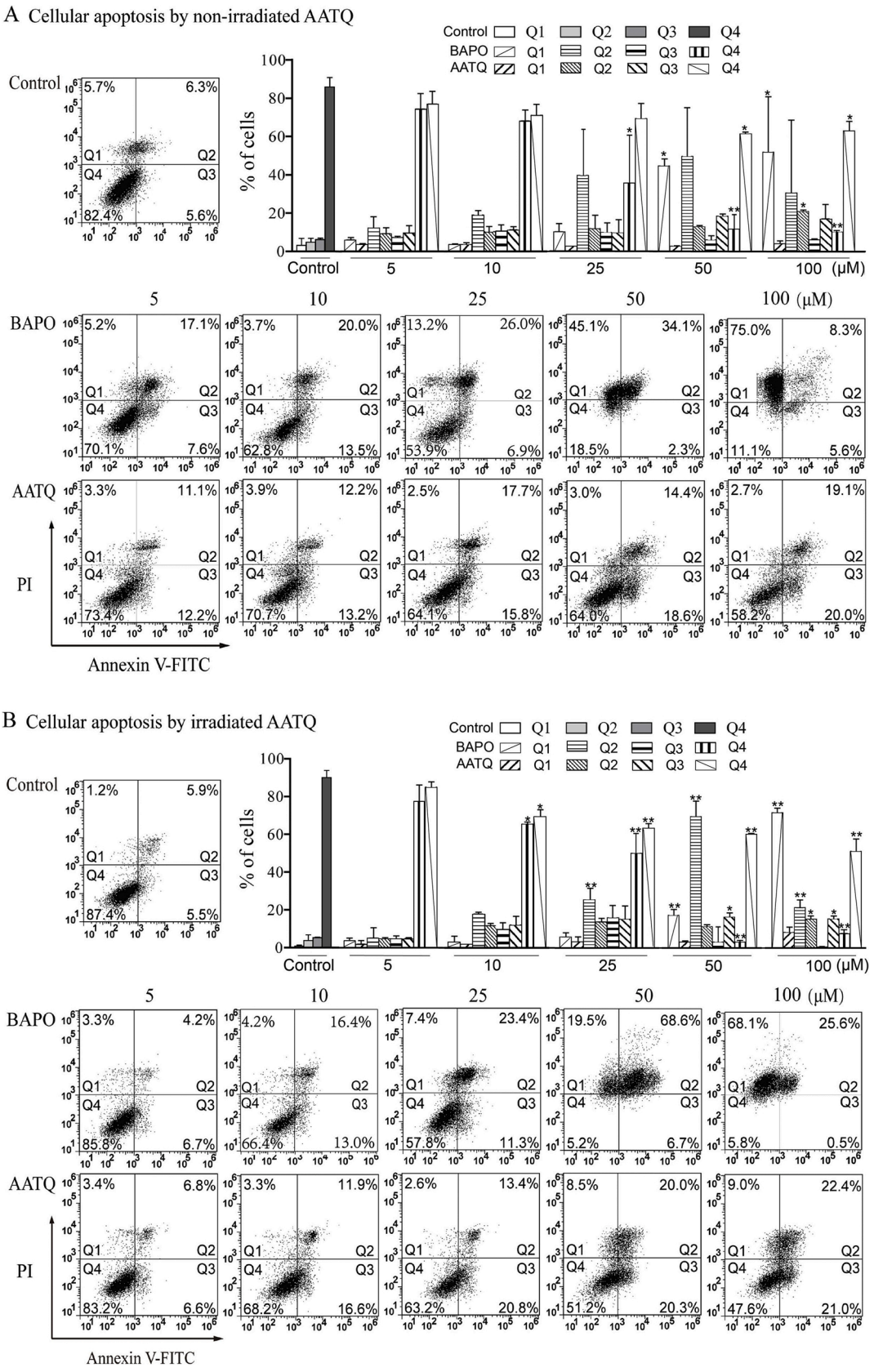

Fig. 7. Induction of apoptosis and necrosis of HEK293T cells by AATQ. Treatment with BAPO used as a positive control. A. HEK293T cells were exposed to photoinitiator AATQ or BAPO used as a positive control for 24 h. They were collected for PI and annexin V dual staining and run with flow cytometry. B. The cell apoptosis was detected after the initiator was exposed to 455 nm LED for 5 min. Quantitatively, the percentage of necrotic cells (Q1), late apoptotic cells and necrotic cells (Q2), early apoptotic cells (Q3) and viable cells (Q4) were calculated. $^{*}p < 0.05$; $^{**}p < 0.01$, *vs.* the control.

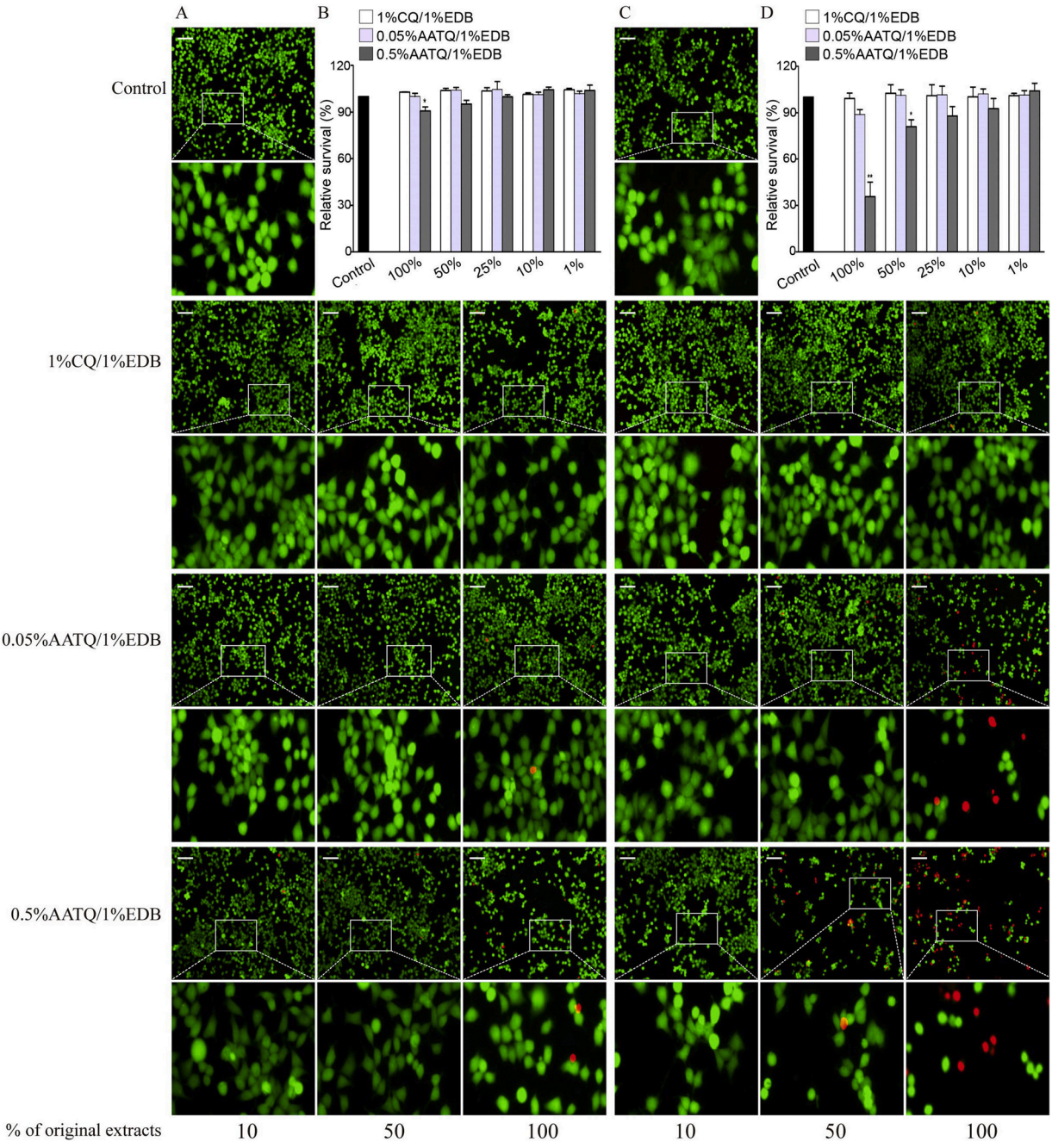

Fig. 8. Viability of HEK293T cells exposed to the composite extracts from AATQ-initiated polymer. MTT assay and cell live/dead staining (different concentration ratios of the original extract: 10, 25, 50, and 100 %) were used to determine the relative metabolic activity and the cell survival of HEK293T, respectively. A-B. The viability of HEK293T cells was observed after a 24 -h exposure culture to the 1-day composite extracts. C-D. The viability of HEK293T cells was observed after a 24 -h exposure culture to the 7-day composite extracts. Error bars are expressed as mean ± SD; Rulers in images: 100 μM.

TPO induced the reduction of the cell number in a dose-dependent manner, and the cytotoxicity was 50–250 times higher than CQ [18]. Therefore, it is necessary to evaluate the cytocompatibility of these materials. In this study, BAPO was selected as a toxic control. Considering that different cell lines may have different sensitivity to materials, three different tissue types of cell lines and a type of primary cells were selected to detect cytotoxicity. And it turns out that HEK293T and BMSCs are more sensitive to these photoinitiators. Previous studies have also shown that six cell lines have different toxic responses to I2959 [1]. This suggests that different tissues in the body have different responses to the toxicity of the initiator.

Cells may undergo apoptosis and necrosis after photoinitiator treatment. To observe changes in cell death patterns after photoinitiator treatment, we performed annexin V/PI analysis. The data have shown that monomers and photoinitiators cause cellular redox imbalance, which leads to apoptosis and DNA damage by increasing ROS levels [20, 21]. Oxidative stress is involved in enhancement of intracellular ROS, resulting in damage to lipids, proteins and DNA, and is associated with numerous diseases [22–24]. CQ can trigger a rapid increase in intracellular ROS, which may eventually lead to mutagenesis [25]. Apoptosis of AATQ-treated cells was detected using sensitive HEK293T. As shown in Fig. 3, AATQ does increase the proportion of apoptosis with increasing concentrations. This indicates that AATQ can cause cell death by promoting apoptosis. In contrast, BAPO is more likely to cause cell

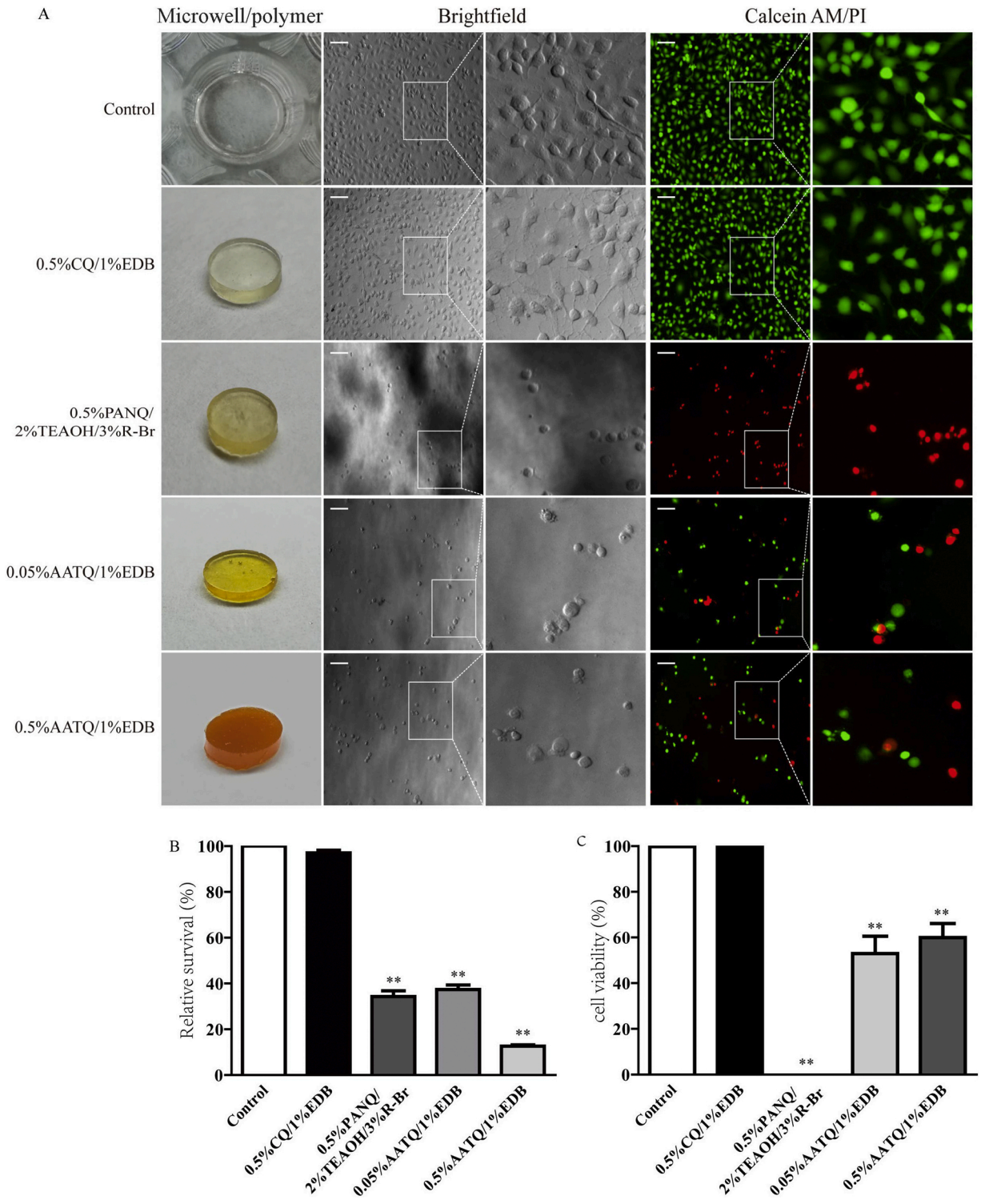

Fig. 9. *In vitro* cell seeding on the surface of polymers. After 24 h of culture, the viability of HUVEC-12 cells seeded on specimens was determined by Calcein-AM/PI staining Calcein-AM stained the living cells green and PI stained the dead cells red. A. Representative Live/Dead images of the cells that were seeded on the surfaces of the specimens (AATQ/EDB (0.5 %/1 % w/w), AATQ/EDB (0.05 %/1 % w/w), PANQ/TEAOH/R-Br (0.5 %/2 %/3 %, wt%) and CQ/ EDB(0.5 %/1 % w/w) in BisGMA/TEGDMA (70 %/30 % w/w)), respectively. B. The metabolic activity of HUVEC12 cells was measured by MTT assay 24 h after cell seeding. C. Cell viability was expressed as a percentage of live cells in total cell count. $^{*}p < 0.05$, $^{**}p < 0.01$ *vs.* the control group; Rulers in images: 100 μM. (For interpretation of the references to colour in this figure legend, the reader is referred to the web version of this article).

necrosis, showing a difference in the way of cell damage. That is, the toxicity mechanism is not exactly the same. The photopolymerization system is actually used in the exposure condition, and the photo-activated initiator may produce increased cytotoxicity. In this experiment, AATQ and BAPO were excited by a blue LED to observe the changed cell responses. The results of MTT showed that the metabolic activities of the cells in the BAPO group before and after irradiation were basically the same, while there was a slight increase in toxicity after AATQ irradiation. This may be due to an increase in the level of active oxygen caused by photoexcitation. Therefore, in development and

research of light triggering, we should not only consider its own characteristics but also pay attention to changes after excitation.

Numerous studies have shown that some common monomers, diluents, photoinitiators and their auxiliaries can cause cytotoxicity, genotoxicity [18,20,21], and apoptosis [26] in various cell types. Thus, monomers that are not completely crosslinked during photopolymerization or incompletely reacted initiators cause certain cytotoxic effects. For example, toxic substances in dental composites can be released into body fluids by hydrolysis and enzymatic degradation as well as mechanical abrasion [27–29]. In this study, photoinitiator PANQ with higher photoinitiating ability than CQ was also used as another control for further understanding a relationship of photoinitiators, their conversion efficiency, non-crosslinked monomers with cytotoxicity and cytocompatibility. PANQ is also an aromatic diketone and its usually used concentration for cell research is 1−10 μM [30–33], showing a rich variety of photochemical characteristics, and its absorption spectrum can reach the visible region [34,35]. It is used as a photoinitiator in the photopolymerization system [36,37]. The applicability of PANQ in experimental dental composites was evaluated, and when tested with Iod or EDB + Iod, materials prepared with CQ present similar conversion efficiency to those prepared with PANQ [38]. Our data show that the product of the 0.5 % AATQ/1 % EDB group appears dark yellow and the 0.05 % AATQ/1 % EDB group pale yellow, suggesting that higher concentration of AATQ would result in more unreacted monomer in the polymer. Therefore, the higher the amount of photoinitiator in the polymerization reaction system, the worse the polymerization effect, and the same is true for some initiators newly designed and synthesized [39]. Notably, the CQ-initiated polymer hardly affects cell viability, while the photocured AATQ polymer would not well support cell growth, but still superior significantly to the PANQ-initiated polymer, on which almost all the cells are dead. PANQ, like AATQ, is also an inclusion in the exhaust gas. It is mainly a sort of quinone chemical existed in diesel exhaust particles, generating reactive oxygen species *in vitro* [40–42]. Thus, it is speculated that the leaching of the uncrosslinked components might mainly contribute to the toxic response, and the reduced conversion rate may result in poor cell compatibility. Another aspect that may affect cellular responses is the polymer network itself, which may have a greater negative impact on cell viability and proliferation [43].

5. Conclusions

In short, AATQ shows some cytotoxicity at a micromolar concentration, which is slightly aggravated after irradiation, but its toxicity is much lower than the widely used BAPO. Its cytocompatibility is superior to PANQ with the similar extent of polymerization in depth within a certain range, but inferior to CQ. Hence, AATQ offers an alternative no matter in application of industrial or biomedical areas, especially in polymerization systems requiring low concentrations of a photoinitiator.

CRediT authorship contribution statement

Feiyue Xing conceived and designed this study. **Shuhui Wang** and **Yongjia Xiong** contributed to the datum acquisition and the draft of this manuscript. **Hailing Zou**, **Jiawen Guo** and **Boning Zeng** participated in the partial experiment. **Feiyue Xing** contributed to the interpretation of the data and the writing of the manuscript. **Feiyue Xing**, **Jing Liu** and **Pu Xiao** revised it. All authors gave final approval and agree to be accountable for all aspects of work ensuring integrity and accuracy.

Declaration of Competing Interest

The authors declare no conflict of interest.

Acknowledgements

This work was supported by the National Natural Science Foundation of China (grant number: 81172824) and Guangzhou City Science and Technology Program Synergistic Innovation Major Project (grant number: 201604020146) to F.Y. Xing.

References

[1] C.G. Williams, A.N. Malik, T.K. Kim, P.N. Manson, J.H. Elisseeff, Variable cytocompatibility of six cell lines with photoinitiators used for polymerizing hydrogels and cell encapsulation, Biomaterials 26 (2005) 1211–1218.
[2] U. Mangal, Y.L. Min, J.Y. Seo, D.E. Kim, J.Y. Cha, K.J. Lee, J.S. Kwon, S.H. Choi, Changes in tribological and antibacterial properties of poly(methyl methacrylate)-based 3D-printed intra-oral appliances by incorporating nanodiamonds, J. Mech. Behav. Biomed. Mater. 110 (2020) 103992.
[3] L. Han, J.L. Xu, X. Lu, D.L. Gan, Z.X. Wang, K.F. Wang, H.P. Zhang, H.P. Yuan, J. Weng, Biohybrid methacrylated gelatin/polyacrylamide hydrogels for cartilage repair, J Mater. Chem. B 5 (2017) 731–741.
[4] W. Bonani, N. Cagol, D. Maniglio, Alginate hydrogels: a tool for 3D cell encapsulation, tissue engineering, and biofabrication, Adv. Exp. Med. Biol. 1250 (2020) 49–61.
[5] S.L. Fenn, T. Miao, R.M. Scherrer, R.A. Oldinski, Dual-cross-Linked methacrylated alginate sub-microspheres for intracellular chemotherapeutic delivery, ACS Appl. Mater. Interfaces 8 (2016) 17775–17783.
[6] S. Dinescu, B. Galateanu, E. Radu, A. Hermenean, A. Lungu, I.C. Stancu, D. Jianu, T. Tumbar, M. Costache, A 3D porous gelatin-alginate-based-ipn acts as an efficient promoter of chondrogenesis from human adipose-derived stem cells, Stem Cells Int. 2015 (2015) 252909.
[7] D.A. Klumpp, Y.L. Zhang, D. Do, R. Kartika, Reactions of acenaphthenequinone and aceanthrenequinone with arenes in superacid, Appl. Catal. A-Gen. 336 (2008) 128–132.
[8] Y.Y. Liu, F.N. Sun, Z.J. He, Recent renewed interest in the classical Kukhtin-Ramirez adducts, Tetrahedron Lett. 59 (2018) 4136–4148.
[9] R. Zhou, L. Han, H.H. Zhang, R.F. Liu, R.F. Li, A Deoxygenative [4+1] Annulation Involving N-Acyldiazenes for an Efficient Synthesis of 2,2,5-Trisubstituted 1,3,4-Oxadiazole Derivatives, Adv. Synth. Cataly. 359 (2017) 3977–3982.
[10] C.A. Jakober, S.G. Riddle, M.A. Robert, H. Destaillats, M.J. Charles, P.G. Green, M. J. Kleeman, Quinone emissions from gasoline and diesel motor vehicles, Environ. Sci. Technol. 41 (2007) 4548–4554.
[11] M. Pardo, F. Xu, M. Shemesh, X. Qiu, Y. Barak, T. Zhu, Y. Rudich, Nrf2 protects against diverse PM2.5 components-induced mitochondrial oxidative damage in lung cells, Sci. Total Environ. 669 (2019) 303–313.
[12] M.I. Gunther, N. Weidner, R. Muller, A. Blesch, Cell-seeded alginate hydrogel scaffolds promote directed linear axonal regeneration in the injured rat spinal cord, Acta Biomater. 27 (2015) 140–150.
[13] L. Zhang, G. Singh, M. Zhang, S.X. Chen, K.G. Xu, P.C. Xu, X.E. Wang, Y.H. Chen, L. Zhang, L. Zhang, Bone marrow-derived mesenchymal stem cells laden novel thermo-sensitive hydrogel for the management of severe skin wound healing, Mater. Sci. Eng. C-Mater. Biol. Appl. 90 (2018) 159–167.
[14] J.L. Ferracane, Elution of leachable components from composites, J. Oral Rehabil. 21 (1994) 441–452.
[15] M. Taira, H. Urabe, T. Hirose, K. Wakasa, M. Yamaki, Analysis of photo-initiators in visible-light-cured dental composite resins, J. Dent. Res. 67 (1988) 24–28.
[16] J. Volk, C. Ziemann, G. Leyhausen, W. Geurtsen, Genotoxic and mutagenic potential of camphorquinone in L5178/TK+/- mouse lymphoma cells, Dent. Mater. 34 (2018) 519–530.
[17] C.T. Meereis, F.B. Leal, G.S. Lima, R.V. de Carvalho, E. Piva, F.A. Ogliari, BAPO as an alternative photoinitiator for the radical polymerization of dental resins, Dent. Mater. 30 (2014) 945–953.
[18] M. Popal, J. Volk, G. Leyhausen, W. Geurtsen, Cytotoxic and genotoxic potential of the type I photoinitiators BAPO and TPO on human oral keratinocytes and V79 fibroblasts, Dent. Mater. 34 (2018) 1783–1796.
[19] S.H. Wang, Y.J. Xiong, J. Lalevée, P. Xiao, J. Liu, F.Y. Xing, Biocompatibility and cytotoxicity of novel photoinitiator pi-conjugated dithienophosphole derivatives and their triggered polymers, Toxicol. In Vitro 63 (2020) 104720.
[20] S. Krifka, C. Seidenader, K.A. Hiller, G. Schmalz, H. Schweikl, Oxidative stress and cytotoxicity generated by dental composites in human pulp cells, Clin. Oral Invest. 16 (2012) 215–224.
[21] D. Manojlovic, M.D. Dramicanin, V. Miletic, D. Mitic-Culafic, B. Jovanovic, B. Nikolic, Cytotoxicity and genotoxicity of a low-shrinkage monomer and monoacylphosphine oxide photoinitiator: comparative analyses of individual toxicity and combination effects in mixtures, Dent. Mater. 33 (2017) 454–466.
[22] C. Holze, C. Michaudel, C. Mackowiak, D.A. Haas, C. Benda, P. Hubel, F. L. Pennemann, D. Schnepf, J. Wettmarshausen, M. Braun, D.W. Leung, G. K. Amarasinghe, F. Perocchi, P. Staeheli, B. Ryffel, A. Pichlmair, Oxeiptosis, a ROS-induced caspase-independent apoptosis-like cell-death pathway, Nat. Immunol. 19 (2018) 130–140.
[23] M. Schieber, N.S. Chandel, ROS function in redox signaling and oxidative stress, Curr. Biol. 24 (2014) R453–462.
[24] O. Shadyro, A. Lisovskaya, ROS-induced lipid transformations without oxygen participation, Chem. Phys. Lipids 221 (2019) 176–183.

[25] J. Engelmann, J. Volk, G. Leyhausen, W. Geurtsen, ROS formation and glutathione levels in human oral fibroblasts exposed to TEGDMA and camphorquinone, J. Biomed. Mater. Res. B Appl. Biomater. 75 (2005) 272–276.
[26] G. Batarseh, L.J. Windsor, N.Y. Labban, Y. Liu, K. Gregson, Triethylene glycol dimethacrylate induction of apoptotic proteins in pulp fibroblasts, Oper. Dent. 39 (2014) E1–8.
[27] H. Schweikl, G. Spagnuolo, G. Schmalz, Genetic and cellular toxicology of dental resin monomers, J. Dent. Res. 85 (2006) 870–877.
[28] M. Wisniewska-Jarosinska, T. Poplawski, C.J. Chojnacki, E. Pawlowska, R. Krupa, J. Szczepanska, J. Blasiak, Independent and combined cytotoxicity and genotoxicity of triethylene glycol dimethacrylate and urethane dimethacrylate, Mol. Biol. Rep. 38 (2011) 4603–4611.
[29] N.J. Walters, W. Xia, V. Salih, P.F. Ashley, A.M. Young, Poly(propylene glycol) and urethane dimethacrylates improve conversion of dental composites and reveal complexity of cytocompatibility testing, Dent. Mater. 32 (2016) 264–277.
[30] T. Matsunaga, T. Kamiya, D. Sumi, Y. Kumagai, B. Kalyanaraman, A. Hara, L-Xylulose reductase is involved in 9,10-phenanthrenequinone-induced apoptosis in human T lymphoma cells, Free Radic. Biol. Med. 44 (2008) 1191–1202.
[31] T. Matsunaga, M. Arakaki, T. Kamiya, M. Haga, S. Endo, Nitric oxide mitigates apoptosis in human endothelial cells induced by 9,10-phenanthrenequinone: role of proteasomal function, Toxicology 268 (2010) 191–197.
[32] N. Hatae, J. Nakamura, T. Okujima, M. Ishikura, T. Abe, S. Hibino, T. Choshi, C. Okada, H. Yamada, H. Uno, E. Toyota, Effect of the orthoquinone moiety in 9,10-phenanthrenequinone on its ability to induce apoptosis in HCT-116 and HL-60 cells, Bioorg. Med. Chem. Lett. 23 (2013) 4637–4640.
[33] K. Kamase, M. Taguchi, A. Ikari, S. Endo, T. Matsunaga, 9,10-Phenanthrenequinone provokes dysfunction of brain endothelial barrier through down-regulating expression of claudin-5, Toxicology 461 (2021) 152896.
[34] D.M. Togashi, D.E. Nicodem, Photophysical studies of 9,10-phenanthrenequinones, Spectrochim. Acta A 60 (2004) 3205–3212.
[35] V.E. Salgado, D. Cavassoni, A.P.R. Goncalves, C. Pfeifer, R.R. Moraes, L. F. Schneider, Photoinitiator system and water effects on C=C conversion and solubility of experimental etch-and-rinse dental adhesives, Int. J. Adhes. Adhes. 72 (2017) 6–9.
[36] J.H. Chen, C.T. Yang, C.H. Huang, M.F. Hsu, T.R. Jeng, Study of optical properties of glass-like polymer material for blue laser holographic optic data storage recording, IEEE T Magn. 45 (2009) 2256–2259.
[37] S.A. Chesnokov, M.Y. Zakharina, A.S. Shaplov, Y.V. Chechet, E.I. Lozinskaya, O. A. Mel'nik, Y.S. Vygodskii, G.A. Abakurnov, Ionic liquids as catalytic additives for the acceleration of the photopolymerization of poly(ethylene glycol dimethacrylate)s, Polym. Int. 57 (2008) 538–545.
[38] P.P.A.C. Albuquerque, M.L. Bertolo, L.M.A. Cavalcante, C. Pfeifer, L.F.S. Schneider, Degree of conversion, depth of cure, and color stability of experimental dental composite formulated with camphorquinone and phenanthrenequinone photoinitiators, J. Esthet. Restor. Dent. 27 (2015) S49–S57.
[39] A. Al Mousawi, P. Garra, X. Sallenave, F. Dumur, J. Toufaily, T. Hamieh, B. Graff, D. Gigmes, J.P. Fouassier, J. Lalevée, Π-conjugated dithienophosphole derivatives as high performance photoinitiators for 3D printing resins, Macromolecules v.51 (no.5) (2018) 11–1821, 2018.
[40] K. Taguchi, M. Shimada, S. Fujii, D. Sumi, X. Pan, S. Yamano, T. Nishiyama, A. Hiratsuka, M. Yamamoto, A.K. Cho, J.R. Froines, Y. Kumagai, Redox cycling of 9,10-phenanthraquinone to cause oxidative stress is terminated through its monoglucuronide conjugation in human pulmonary epithelial A549 cells, Free Radical Bio. Med. 44 (2008) 1645–1655.
[41] K. Taguchi, Oxidative stress-dependent cellular toxicity and cytoprotection during exposure to 9,10-phenanthraquinone, a component of diesel exhaust particles, J. Health Sci. 55 (2009) 347–350.
[42] R. Sugimoto, Y. Kumagai, Y. Nakai, T. Ishii, 9,10-Phenanthraquinone in diesel exhaust particles downregulates Cu,Zn-SOD and HO-1 in human pulmonary epithelial cells: Intracellular iron scavenger 1,10-phenanthroline affords protection against apoptosis, Free Radical Bio. Med. 38 (2005) 388–395.
[43] N.J. Lin, L.O. Bailey, M.L. Becker, N.R. Washburn, L.A. Henderson, Macrophage response to methacrylate conversion using a gradient approach, Acta Biomater. 3 (2007) 163–173.